# MICROWAVE PHASE SHIFTERS

## SCANNING ARRAY ANTENNA APPLICATIONS

Mechanical motion necessary for antenna scanning was perceived to be slow and unreliable. For this reason the microwave industry developed an intense interest in phased array antennas, primarily for military but also for commercial applications. The antenna's radiated wavefront would be steered by thousands of individual radiators, roughly one for each half wavelength square area of the radiating aperture. Each radiator would be controlled by a solid state (either semiconductor or ferrite) phase shifter, having low insertion loss and 0° to 360° of phase shift. For computer control the phase shift would be accomplished in binary bits. Thus a 3-bit phase shifter would have a 180°, a 90°, and a 45° section and these could be used to provide 0° to 315° control in 45° steps (the last step to 360° is not needed, being equivalent to 0° in the steady state). The antennas would be more expensive, both because of their need for numerous control elements (a circular aperture 30 wavelengths in diameter requires about 2,500 elements) and the fact that, since a phased array provides only about ±45° of steering, four separate apertures are needed for 360° azimuthal coverage. But they would be fast and nearly failsafe, since a failure of a few elements would result in but "graceful degradation" of the system.

J. Webster (ed.), *Wiley Encyclopedia of Electrical and Electronics Engineering*. Copyright © 1999 John Wiley & Sons, Inc.

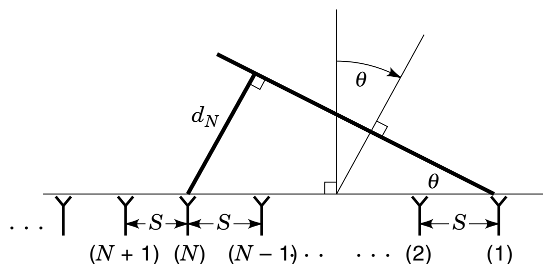


**Figure 1.** A linear phased array steered with time delay.

Ideally time delay (Fig. 1) is used to steer an array of antenna elements, and a two-dimensional array uses total time delay equal to that required for both azimuth and elevation steering. When time delay is used, the steering is frequency independent, very desirable for a broadband antenna. However, the time delay required, equivalent to 70% of the antenna width for 45° beam steering along either of the antenna's steering axes, can amount to thousands of degrees of control. Instead, phase control is used. The requisite time delay is first calculated by the beam steering computer and then all integer wavelengths dropped. The residue in degrees is then provided (to within one-half of the least significant bit) as a command to the binary bit phase shifter. In some cases, groups of adjacent phase shifters (subarrays) may employ time-delay steering to enhance antenna bandwidth performance.

Over the last four decades there has been a keen competition between the rival technologies, semiconductor and ferrite, to achieve the phase control. The semiconductor devices and their circuitry are generally faster switching and inherently reciprocal (having the same phase shift on transmit as receive), a useful antenna property. Being switches, their phase control is essentially temperature invariant, and the circuits more easily reproduced. Driver circuits, which interface the microwave control circuit to the array antenna beam steering computer, are very simple for the semiconductor phase shifter. However, semiconductors are discrete and small switching elements, and thereby limited in their peak power-handling capacity. Furthermore, their insertion losses increase with frequency.

Ferrites are a controllable propagation medium for microwaves and thus have more volume and a higher power-handling capacity. Properly designed, they have low losses at higher microwave frequencies and, for certain circuit configurations, can be made reciprocal, even though propagation through the medium itself is nonreciprocal. Considerable attention must be given to the ferrite's flux driver circuitry to achieve reproducible binary phase control from unit to unit and over temperature and bias supply voltage changes. In fact, taking its driver circuit into account, a ferrite phase shifter typically includes more semiconductors than does a semiconductor phase shifter.

This section treats the semiconductor phase shifter. While they could be built using a variety of semiconductors, diodes, bipolar and field effect transistors, the principal development was with silicon *pin* diodes because of their relatively low cost, high microwave $Q$, and inherent inertia to changes in characteristics with applied microwave (RF) excitation. To appreciate this requires some description of the *pin* diode.

## THE PIN DIODE

Generally, semiconductor *pn* junctions have rapid response to an applied voltage and even can be used to rectify an RF signal for detection purposes. However the *pin* has a high resistivity (intrinsic), undoped region between its $p$ and $n$ zones. The result is that holes and electrons which are injected from the $p$ and $n$ zones under forward bias move by diffusion into the $i$ region, where they serve as mobile charge not unlike electrons in copper, rendering the $i$ region conductive to an applied RF signal. Electrons and holes can combine with one another, resulting in carrier death, but to do so they must give up energy equal to the energy difference between the valence and conduction bands (the bandgap). For silicon this is 1.1 electron volts, and such a drop in energy requires an energy emission, if performed in one step, of a photon of visible light. We do not observe silicon to be glowing with such light emission, because such a transition is very unlikely. Put another way, the lifetime of an electron–hole pair is long, tens of microseconds for the resistivities obtained in practical diodes. The "staircase" of energy steps resulting from impurities and stresses in an otherwise ideal silicon crystal produce a far more likely energy transition between bands, consequently lower carrier lifetime.

The charge storage in a *pin*'s $i$ region is equal to the product of the lifetime and the forward bias (Fig. 2). Thus, for example, a 1,000 V breakdown *pin* diode might have a 5 $\mu$s lifetime and be biased with a current of 100 mA, resulting in a stored charge of 0.5 $\mu$C. When a 1 GHz sinusoid having a peak current of 50 A is applied to the diode, it causes a peak-to-peak charge movement of less than 0.025 $\mu$C, less than 5% of the charge stored by the bias. The result is that the diode appears to be a low value of resistance throughout the entire RF sinusoid.

The same diode, when operated at a reverse bias of −100 V, is able to sustain, without conduction, an applied RF sinusoid of 1,000 V peak. This is because the diode requires a microsecond or more to establish a conducting state in the $i$ re-

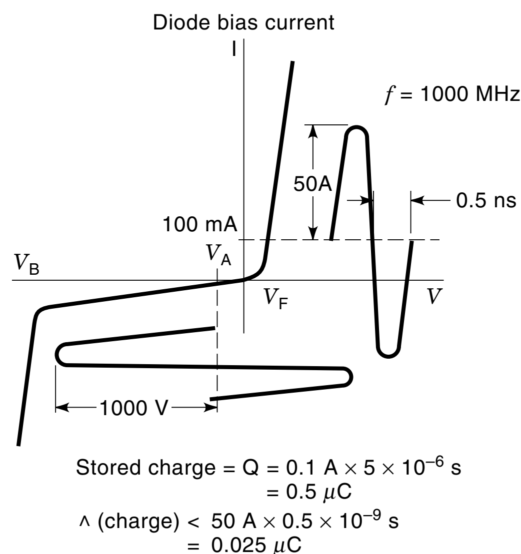


**Figure 2.** Example comparing charge stored in a *pin* by the bias to the charge movement due to a high-level RF signal.

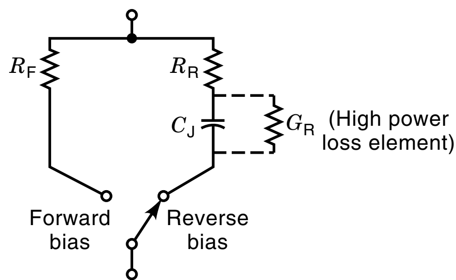


**Figure 3.** *pin* diode chip equivalent circuit.

gion, much longer than the half nanosecond forward-going voltage duration of a 1 GHz sinusoid.

Well-made *pin* diodes enjoy a bulk breakdown voltage of about 10 V/$\mu$m (250 V/mil) of $i$ region width. It is this bulk breakdown that determines the *pin*'s ability to sustain RF voltage. Conduction due to impact ionization in the $i$ region can occur rapidly, even within an RF half cycle.

Ryder (1) has likened the bias on a *pin* diode to the "large signal" and the RF as the "small ac component," the truth of which is evident from the relative magnitudes of the charges related to each. The result of this remarkable behavior is that the *pin* can control tens of kilowatts of RF power, using only fractions of a watt of bias power.

Using the charge control approach for determining the RF properties the RF resistance, $R_i$, of the *pin* under forward bias is found to be [(2), p. 62]

$$R_i = W^2/(2\mu_{AP}\tau i_0) \quad (1)$$

where, in the *pin* diode's $i$ region, $W$ = the $i$ region thickness; $\mu_{AP}$ = the ambipolar mobility (the effective average velocity per unit applied electric field of the holes and electrons); $\tau$ = the average lifetime of holes and electrons; and $i_0$ = the forward bias current.

For the *pin* used in the example of Fig. 1, $W$ = 100 $\mu$m (4 mils), $\mu_{AP}$ = 610 cm$^2$/V (in silicon), $\tau$ = 5 $\mu$s, and a suitable bias current is 0.1 A, resulting in an RF resistance of only 0.16 Ω. To $R_i$ must be added the ohmic contributions of the $p$ and $n$ regions of the diode, as well as the contact resistances of the diode package. Even so, the total forward biased resistance, $R_F$, is usually 0.5 Ω or less. Interestingly, $R_i$ is not dependent upon $i$ region diameter, $D$, directly. However, indirectly it is, since smaller diameter diodes have lower $\tau$, because carriers, on average, are closer to the $i$ region boundaries at which recombination can more readily take place.

PIN diode area $A$ does relate to the junction capacitance, $C_J$, which follows the parallel plate formula fairly closely.

$$C_J = \epsilon_R \epsilon_0 A/W \quad (2)$$

At low frequencies, say 1 MHz, a $C$ change between zero and reverse bias voltage is observable; however, at RF, it is the minimum capacitance which is experienced due to the dielectric relaxation of the $i$ region (2). With the high dielectric constant of silicon ($\epsilon_R$ = 11.8), there is little fringing of the electric field.

In series with this capacitance is a resistance $R_R$ (not necessarily equal to $R_F$), which is determined by measurement. An RF figure of merit for the *pin* is the switching cutoff frequency, $F_{CS}$ given by

$$F_{CS} = 1/(2\pi C_J \sqrt{R_F R_F}) \quad (3)$$

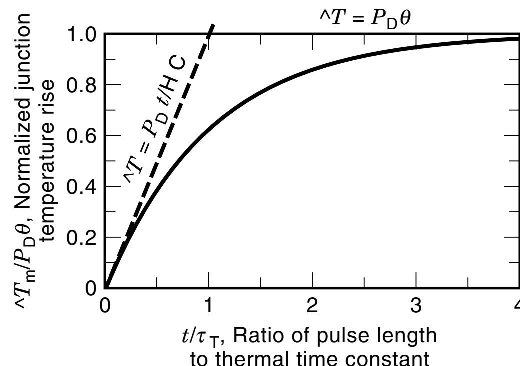


**Figure 5.** General pulsed temperature rise profile of a *pin* diode, using the minimum time constant model.

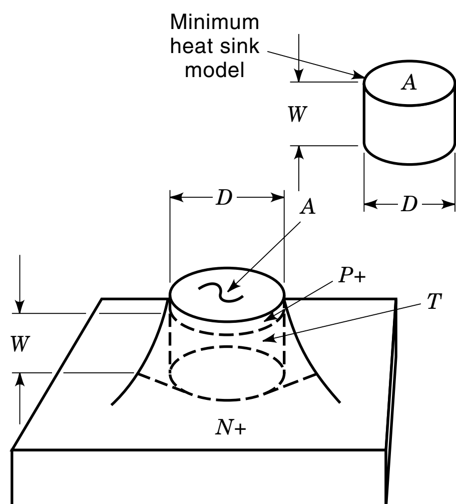


**Figure 4.** *pin* model used for heat sinking calculation.

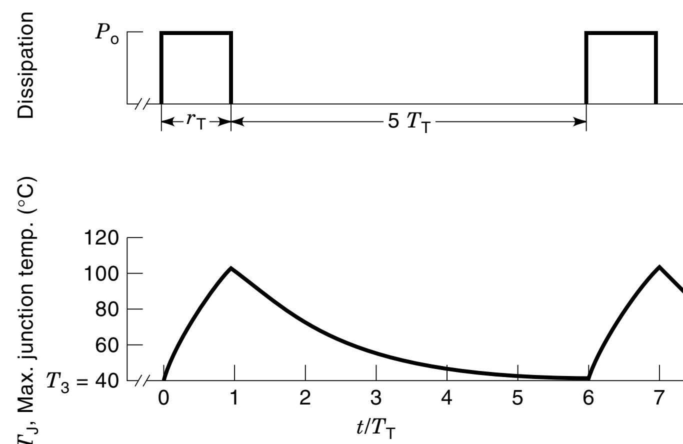


**Figure 6.** Sample estimate of *pin* junction temperature during a train of power dissipating pulses.

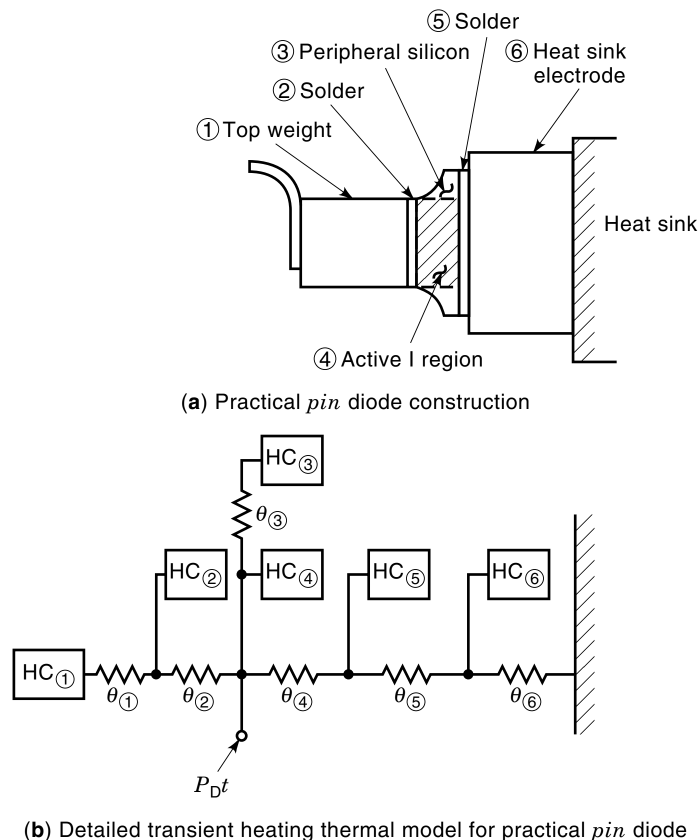


**Figure 7.** Constructional *pin* detail and its thermal model.

As will be described later, the $F_{CS}$ value permits a prediction of the minimum insertion loss to be obtained in a phase shifter, switch, or duplexer circuit, even before the circuit configuration has been specified [(2), Chap. 5]. The RF equivalent circuit of the *pin* chip in its two bias states is shown in Fig. 3. Package capacitance and inductance must be added for a complete packaged diode. For our sample diode, having a junction diameter of 0.49 mm (19 mils), $C_J$ = 0.2 pF.

When suitably soldered either into a package or onto a good heat sink, it is found that the junction temperature rise of our sample diode is about 15°C per watt of power dissipated in the junction. Equivalently stated, its thermal resistance, $\theta$ = 15°C/W. In pulsed RF power applications there may be insufficient time during the pulse for thermal equilibrium to be reached. The junction temperature may rise linearly and the diode *i* region, small as it may seem, must sink the heat dissipated until it can flow out through the thermal resistance path (Fig. 4). The heat capacity HC of the *i* region is given by

$$\text{HC} = (\text{specific heat}) \times (\text{density}) \times (\text{volume}) \tag{4}$$

which, for a silicon *pin* = (0.74 J/g-°C) × (2.43 g/cm$^3$) × ($\pi D^2 W/4$).

For our sample diode, having $D$ = 49 mm (19 mils) and $W$ = 100 μm (100 mils), HC = 34 μJ/°C. This is indeed a small heat capacity, yet it implies that, for a given temperature rise, the *pin* could dissipate nearly seven times as much power for 1 μs as it could sustain with continuous dissipation. Furthermore, this HC calculation is conservative, because it ignores the heat sinking capacity of the bond wires and the *p* and *n* portions of the diode that are in intimate contact with the *i* region. The product of HC and $\theta$ gives the thermal time constant, $\tau_T$, from which the temperature rise, $\Delta T_J$ of the *i* region can be estimated for any pulse length, *t*, of power dissipation, $P_D$. Thus,

$$\tau_T = (\text{HC})(\theta) \tag{5}$$

$$\Delta T_J = P_D \theta (1 - e^{t/\tau_T}) \tag{6}$$

The temperature rise is shown graphically in Fig. 5. For the sample diode the minimum $\tau_T$ is 500 μs. If a safe temperature rise is considered to be 100°C, then the diode could dissipate

**Table 1. Typical Parameters of Available PIN Diodes**

| Symbol | Electrical and Physical Parameters | Units | MA-47890 | MA-47891 | MA-47892 | MA-47893 | MA-47894 | MA-47895 | MA-47896 | MA-47897 | MA-47898 | MA-47899 | MA-47152 | MA-47154 | MA-47156 |
|---|---|---|---|---|---|---|---|---|---|---|---|---|---|---|---|
| (1) $W$ | *i* region width | μm (mils) | 150 (6) | 100 (4) | | | | 50 (2) | | | 25 (1) | | 12 (0.5) | 6 (0.25) | 2 (0.1) |
| (2) $V_{BB}$ | Bulk breakdown voltage | kV | 1.8 | 1.2 | | | | 0.6 | | | 0.3 | | 0.15 | 0.07 | 0.03 |
| (3) $D$ | *i* region effective diameter | mm (mils) | 2.3 (92) | 1.56 (61) | 1.10 (43) | 0.49 (19) | 0.35 (14) | 0.65 (26) | 0.35 (14) | 0.25 (10) | 0.25 (10) | 0.18 (7) | 0.12 (5) | 0.09 (3) | 0.05 (2) |
| (4) $C_j$ | Junction capacitance | pF | 3 | 2 | 1 | 0.2 | 0.1 | 0.7 | 0.2 | 0.1 | 0.2 | 0.1 | 0.1 | 0.1 | 0.1 |
| (5) $T_w$ | Average carrier transit time | ns | 8500 | 3800 | | | | 950 | | | 250 | | 55 | 14 | 1.5 |
| (6) $I_F$ | Typical bias: Forward | mA | 250 | 150 | 100 | | | 50 | | | 25 | | 25 | 25 | 25 |
| (7) $V_R$ | Typical bias: Reverse | V | 200 | 100 | | | | 50 | | | 25 | | 10 | 10 | 10 |
| (8) $R_F$ | Forward resistance at 1 GHz at $i_F$ | Ω | 0.2 | 0.3 | 0.4 | 0.8 | 1 | 0.4 | 0.7 | 1 | 0.9 | 1 | 1 | 1 | 1 |
| (9) $R_R$ | Reverse resistance at 1 GHz at $V_R$ | Ω | 0.2 | 0.3 | 0.5 | 3 | 6 | 0.6 | 3 | 4 | 2 | 4 | 4 | 4 | 3 |
| (10) $f_C$ | Cutoff frequency (reverse bias) | GHz | 250 | 250 | 300 | 250 | 250 | 350 | 250 | 400 | 400 | 400 | 400 | 400 | 550 |
| (11) $f_{CS}$ | Switching cutoff frequency | GHz | 250 | 250 | 350 | 500 | 600 | 350 | 550 | 700 | 600 | 800 | 800 | 800 | 800 |
| (12) τ | Carrier lifetime at 10 mA | μs | 15 | 8 | 5 | 4 | 3 | 2 | 1.5 | 1 | 0.8 | 0.5 | 0.2 | 0.1 | 0.02 |
| (13) θ | Thermal Resistance | °C/W | 1.5 | 3 | 4 | 15 | 25 | 7 | 12 | 15 | 15 | 25 | 30 | 35 | 40 |
| (14) HC | *i* region heat capacity | μJ/°C | 1100 | 340 | 170 | 34 | 17 | 30 | 8 | 4 | 2 | 1 | 0.2 | 0.06 | 0.007 |
| (15) $\tau_t$ | Minimum thermal time constant | μs | 1650 | 1000 | 680 | 500 | 425 | 210 | 96 | 60 | 30 | 25 | 6 | 2 | 0.3 |

Offered by the M/A-COM Division of AMP Inc. in Burlington, MA.

6.6 W continuously, 16 W for 500 $\mu$s, 66 W for 50 $\mu$s, and so forth. Following the pulse, the diode cools during the interpulse periods with the same thermal time constant (Fig. 6).

This same reasoning could be applied to develop a more complete thermal model of the diode, which includes its thermal surroundings. Figure 7 shows a more representative model of the diode, with its thermal elements and that of the packaging materials. Generally, however, the simple conservative model is sufficient to estimate the maximum temperature rise to be expected from a given pulsed power dissipation.

A representative listing of a wide range of *pin* diodes is shown in Table 1. Given these parameters, it is possible to estimate most of the performance of a variety of RF phase shifter, switch, and duplexer circuits, even before the circuits themselves are specified.

## LOADED LINE PHASE SHIFTER

A diode phase shifter is a device whose primary function is to change, by means of a control bias, the propagation phase of a microwave signal. Most switches, attenuators, limiters, and duplexers introduce phase shift, although not usually by design. Moreover, since any reactance placed in series or shunt with a transmission line introduces phase shift, the possibilities for phase shift networks are unlimited. However, adding the requirement that the device has minimum insertion and reflective losses reduces the selection of practical circuits.

Most think of switching between circuit paths as a direct means of phase shift (Fig. 8). Actually this is a switched time delay circuit, producing phase shift that is linearly proportional to frequency. This might seem all the more desirable, since it could lead to broadband array antenna steering. However, in practice, the switching between paths is accomplished with limited isolation of the nonselected path. Figure 9 shows how the loss can increase dramatically when the "off" arm resonates.

While time delay circuits have a place, they are not efficient. All of the RF power must be switched between paths and four diodes minimally are required to do this. The insertion loss is the same for all bits, whereas in a phase shifter circuit, only two diodes are required per bit and the diode loss is much less for small phase shift bits. Accordingly, we shall omit further discussion of time delay circuits and proceed to phase shifters (which, generally, do not have linearly increasing phase change with frequency).

Initially it was thought that very high power phase shifters would be required. In fact, the author conducted a Navy-sponsored project, whose objective was a 100 kW peak power phase shifter—an objective that was met and applied to a high power array! The key to the development was the recognition that, since numerous diodes would be required for very high power, each contributing a small amount of the total phase shift required, a circuit lightly coupling the diodes to the propagating wave was needed.

The solution was the transmission phase shifter (Fig. 10), in which pairs of diode switched susceptances load the transmission line. The spacing of the susceptances, about 90°, is selected to cause mutual cancellation of their reflections. The magnitude of the susceptances is made small (less than 0.4 $Y_0$), and so the diodes are subjected to relatively small RF currents and voltages, producing low dissipation in each di-

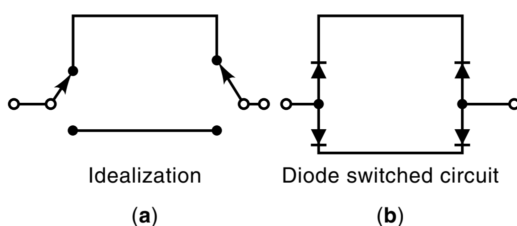


**Figure 8.** Schematic for switched delay line phase shifter.

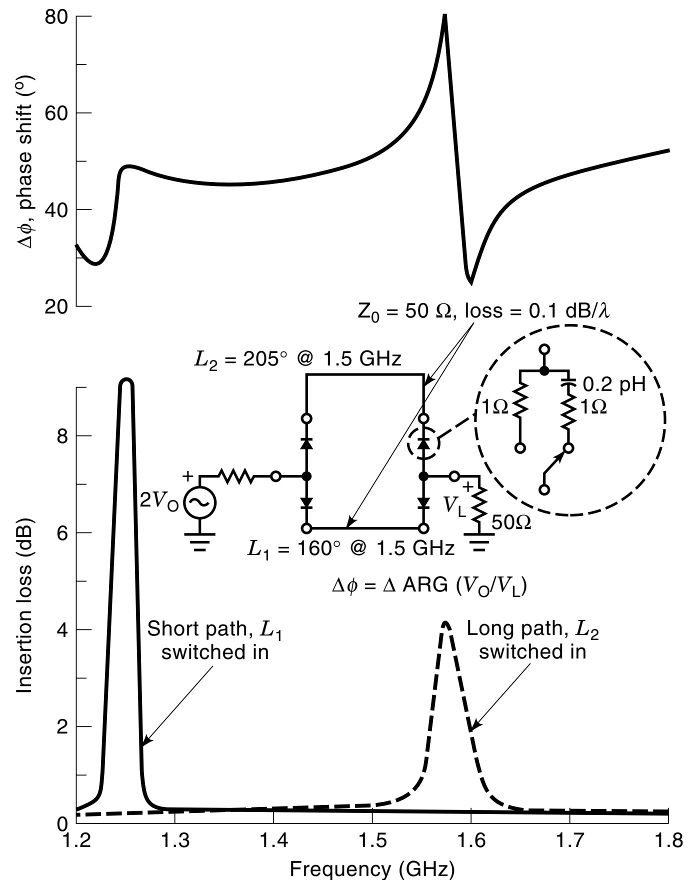


**Figure 9.** Switched path circuit example demonstrating loss resonances.

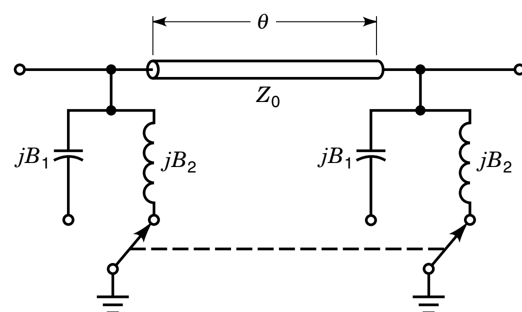


**Figure 10.** Switched transmission phase shifter section, also called the *loaded line phase shifter*.

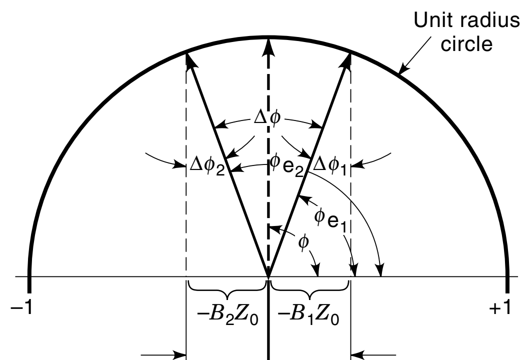


**Figure 11.** Graphical representation of the loaded line phase shifter's change in electrical length caused by switching the loading susceptances.

ode. This enhances both power handling as well as insertion loss performance.

This loaded line section has an equivalent circuit [(2), p. 410] consisting of a uniform line section of new characteristic admittance, $Y_E$, and electrical length, $\theta_E$, related to the loaded line's admittance, $Y_O$, and electrical length, $\theta$, by

$$\cos\theta_E = \cos\theta - (B/Y_O)\sin\theta \tag{7}$$

$$Y_E = Y_O[1 - (B/Y_O)^2 + 2(B/Y_O)\cot\theta]^{1/2} \tag{8}$$

Consider Eq. (7) first. If the line loading susceptance is somehow switched by the *pin* diode between equal magnitude and opposite sign susceptors, $B_1$ and $B_2$, then the electrical length of the loaded line is described by the vector diagram in Fig. 11.

Notice from Fig. 11 that when $\theta = 90°$ the sine of the phase shift, $\Delta\varphi/2$, produced by each of the equal susceptances, $B_i$, is equal to the normalized susceptance term $BZ_O(Z_O = 1/Y_O)$. Then, approximating the sine by its angle, the total phase shift in radians obtained by switching between $B_1$ and $B_2$ is given by

$$\Delta\varphi \cong (B_2 - B_1)Z_O \tag{9}$$

For example, if the normalized susceptances switch between plus and minus 0.2, then the phase shift is 0.4 radians, near 22.5°, a sixteenth of a wavelength. The respective four bits of a phase shifter can be made up of 1, 2, 4, and 8 such sections in cascade.

But, the reader may ask, suppose that the individual reflections from each section, although small in themselves, combine when 15 such sections are cascaded to produce very large reflection and with it high mismatch loss.

Such is not the case. Referring to Eq. (8) and applying the values $\theta = 90°$ and $|B_iZ_O| = 0.2$, gives $Y_E = 0.98Y_O$. This is true for either positive (capacitive) or negative (inductive) line loading. Thus, even as the phase length of the section changes, its characteristic admittance does not. Nor is its value very different from $Y_O$. Accordingly, an arbitrarily long cascade combinations of such sections would not result in a VSWR larger than 1.04, provided that there are no line sections intervening between the phase shift sections. Even this small mismatch could be further compensated by installing a quarterwave line of admittance $1.02Y_O$ at each end of the phase shifter cascade. This inherent match of the loaded line phase shifter is one of its most useful attributes.

It now remains to design the line loading circuits, such that a two-state diode can yield the ±0.2 normalized susceptance switching. The first circuit approach used shunt stubs, whose length was varied by *pin* diode switches (Fig. 12). The diodes were similar to the 0.2 pF, 4 mil I region model described in Table 1. The line lengths $\alpha_1$ and $\alpha_2$ were adjustable. The phase shift was proportional to $\alpha_1$ while the average of the two lengths was adjusted to control the transmission match. With 5° of phase shift per stub pair, a level of 140 kW peak power was sustained with 0.001 duty cycle, 5$\mu$-sec-long

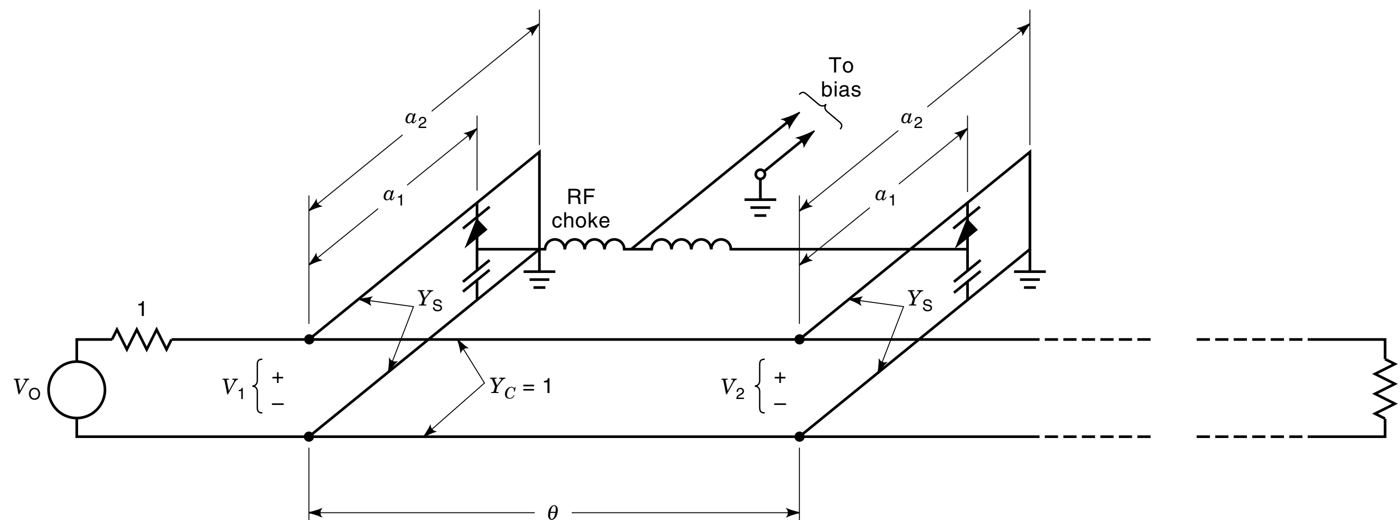


**Figure 12.** Equivalent circuit for one section of the switched stub, loaded line phase shifter tested at 1,300 MHz under high peak power.

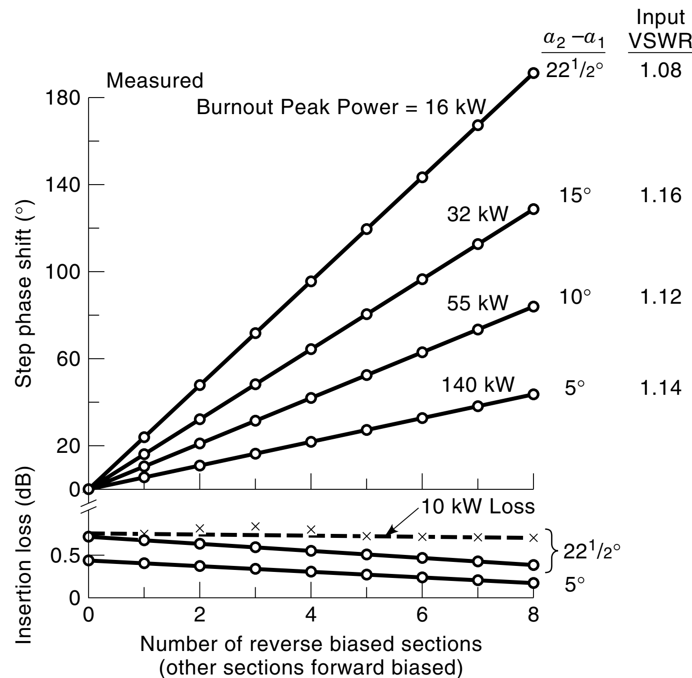


**Figure 13.** L-band measurements of phase shift, insertion loss, and ultimate peak power capability of the switched stub, loaded line phase shifter. Varying switched stub lengths ($\alpha_2$ and $\alpha_1$) produced the different phase shift values and adjusted transmission match.

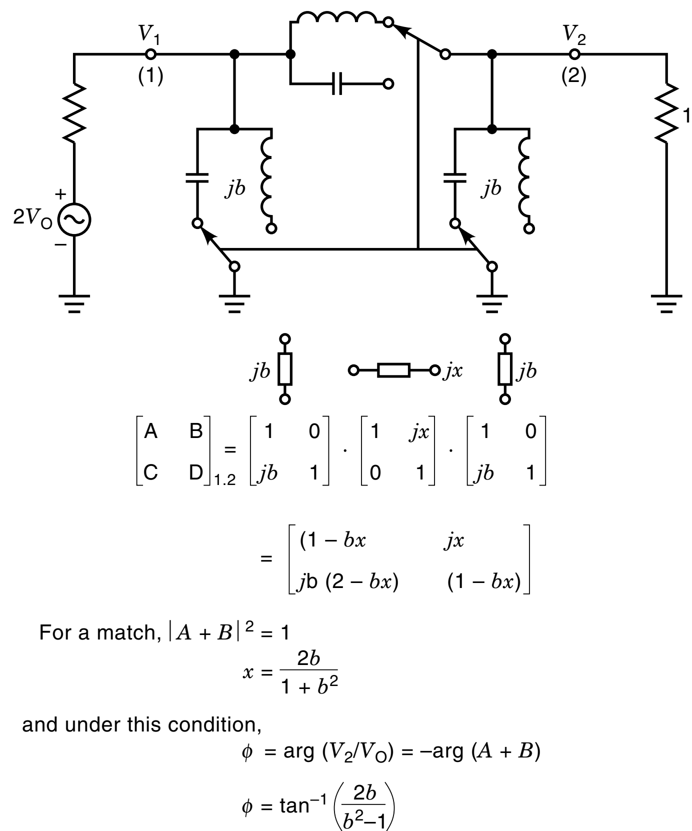


**Figure 14.** The lumped element $\pi$ configuration phase shifter.

pulses at 1,300 MHz. There were eight sections in the experimental model and the results are shown in Fig. 13.

The maximum powers listed are those that cause or nearly cause burnout, usually occasioned by voltage breakdown of the *pin* diodes in the reverse biased state. For *pin*s, as well as all semiconductors, reliable operation requires a rating that imposes only 50% of this maximum voltage stress on the semiconductor. Since power is related to the square of voltage, this means devices need be rated at one-fourth the power level, which would cause immediate failure.

For microwave phase shifters this is especially useful in the event of a short-circuited output, which could nearly double the voltage stress on its diodes. Such a short can result from an arc over or damaged radiating element, even a disconnected output. Indeed, a customary acceptance test for a high-power-control device is operation into a short-circuited load, which is varied through all phases. Given this derating, very high reliability of *pin* phase shifters is experienced, as is necessary in an array antenna.

While it is true that no practical phased array could radiate such levels (a 2,500 element array using 35 kW phase shifters would radiate 87 MW peak power), this result is significant, because single-pole double-throw switches can be constructed by installing such phase shifters between 3 dB hybrid couplers, allowing, for example, the full output power of a radar to be switched between alternate antennas.

The loaded line approach was extended to 3 GHz in a circuit in which the diode's own capacitance terminates the quarterwave shunt stub. Switching between forward and reverse bias changed between $-j50\ \Omega$ (the diode has about 3 pF capacitance) and its forward resistance of 0.5 Ω. Adjusting the shunt stub impedance produced as much as 45° phase shift per pair and a maximum RF peak power of 70 kW [(2), p. 429]. This phaser was used in the US Safeguard system, of which only a prototype system was built.

## LUMPED ELEMENT PHASE SHIFTERS

If the quarterwave section of line in the loaded line section is replaced with a diode switchable reactance (Fig. 14), the lumped element, *high-pass-low-pass* $\pi$ circuit is obtained, which can yield up to 180° of phase shift. A similar tee configuration (2) is also practical. These circuits are advanta-

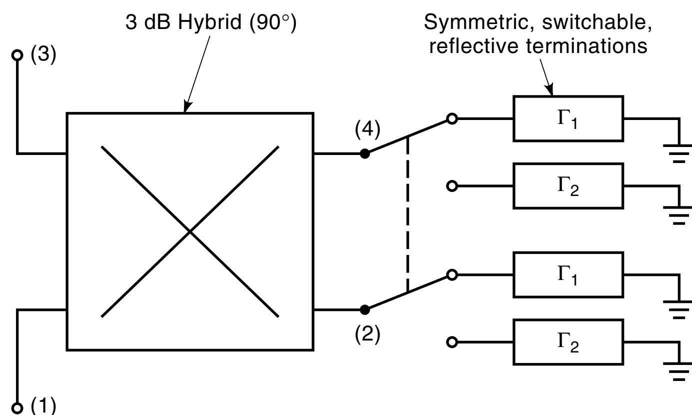


**Figure 15.** The reflection phase shifter circuit employing a coupler to achieve matched two-port transmission.

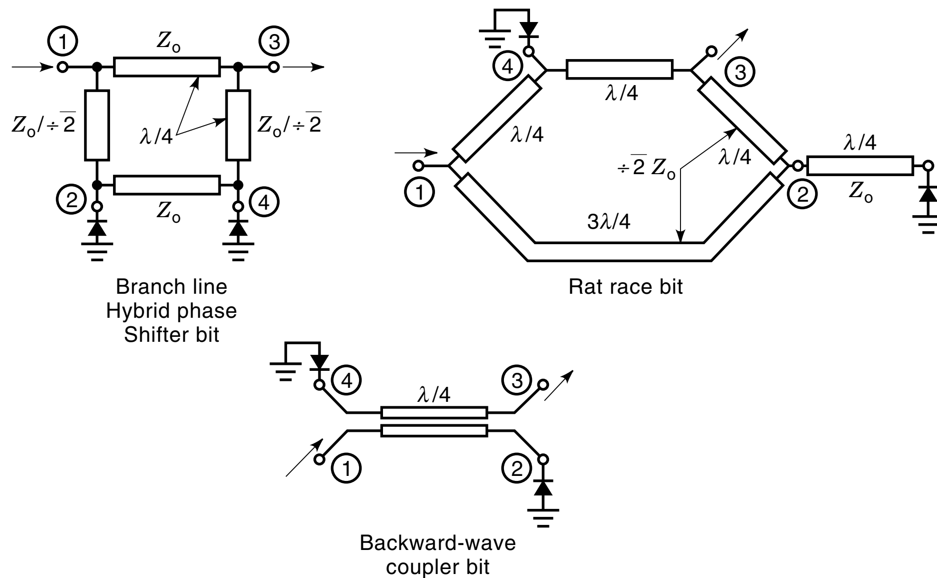


**Figure 16.** Methods of realizing 3 dB, 90° couplers.

geous in integrated circuit applications, because they employ a minimum of switching elements and no space-consuming distributed elements.

For modest power levels, the most common diode phase shifter configuration is the reflection circuit, employing a 3 dB, 90° coupler (Fig. 15). The coupler can be realized in numerous ways, three of which are shown in Fig. 16. The operation of the coupler is to convert the pair of variable phase reflection circuits containing *pin* diodes into a matched two-port network, having the reflection angle change of the terminations.

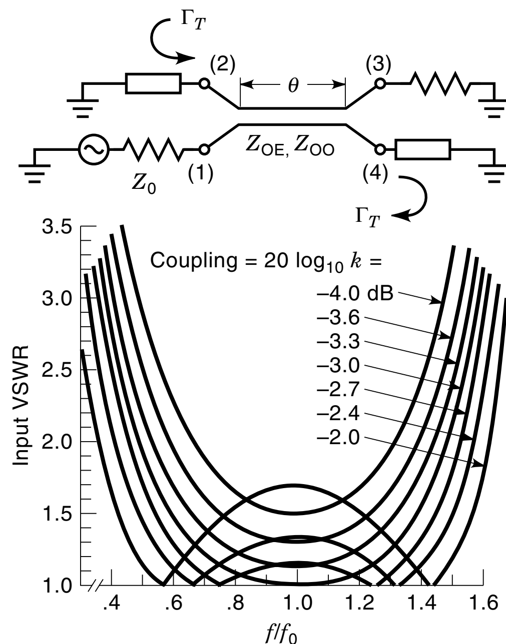


**Figure 17.** VSWR performance with frequency for a coupled line hybrid coupler terminated in symmetric reflections for various coupling values. Note that the −2.4 dB coupler would operate with a maximum VSWR of 1.35 over a band of 0.5 $f_0$ to 1.5 $f_0$, a 3 to 1 frequency range. ($f_0$ is the frequency at which the coupling section is 90° long).

This operation can be explained based on the coupler's operation. Consider the backward wave (hybrid coupler) circuit at the bottom of Fig. 16. Power enters the coupler at port 1 and divides evenly to exit at ports 2 and 4. The wave exiting port 4 has an additional 90°. On encountering the reflective circuits at ports 2 and 4, all energy reenters the coupler, but due to the second 90° phase difference in the signals on this second pass, they cancel at the input (port 1), but add perfectly at the normally decoupled port 3.

This operation requires perfectly even power split and 90° phase difference. The backward coupler (but not the other types shown) has the remarkable property that the 90° phase difference prevails at all frequencies [(2), p. 194]. Of course, the power split varies with frequency, being equal at only one frequency (or two frequencies if the design is overcoupled at the center frequency). Nevertheless, more than octave bandwidth (Fig. 17) with modest VSWR can be obtained with a single coupled line section, even more bandwidth with multistage couplers.

As was true of the loaded line circuit, there are numerous ways to configure the *pin* in a reflection circuit to yield any desired phase shift. However, regardless of what configuration is used, if the circuit is designed to present to the *pin* its maximum sustainable RF voltage, $V_M$, in the reverse biased state and the maximum sustainable RF current $I_M$ in the forward biased state, Hines (3) showed that the maximum

**Table 2. Limits of Power Handling and Insertion Loss ($P_D/P_A$) for Transmission and Reflection Phase Shifters**

| | Power | Loss |
|---|---|---|
| Reflection Circuit | $P_M = \dfrac{V_M I_M}{4\sin(\Delta\phi/2)}$ | $\dfrac{P_D}{P_A} \approx 4\left(\dfrac{f}{f_{cs}}\right)\sin\left(\dfrac{\Delta\phi}{2}\right)$ |
| Transmission Circuit | $P_M = \dfrac{V_M I_M}{2\tan(\Delta\phi)}$ | $\dfrac{P_D}{P_A} \approx 2\left(\dfrac{f}{f_{cs}}\right)\tan(\Delta\phi)$ |
| | | $10f < f_{cs}$ |

$f_{cs} = \dfrac{1}{2\pi c_J\sqrt{R_F R_R}}$

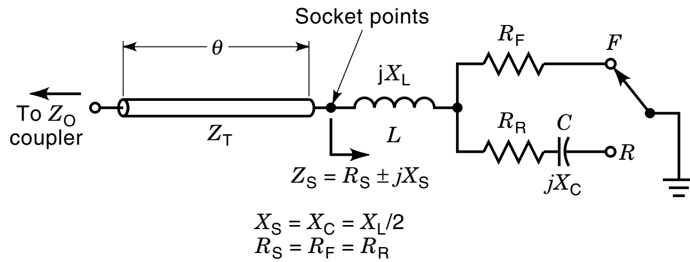


**Figure 18.** The loss equalized phase shifter termination with series inductor and quarterwave transformer to adjust phase shift value.

power $P_M$ sustainable when the circuit yields a phase shift $\Delta\varphi$ is as shown in Table 2. Similarly, if the circuit is designed such that the fraction of incident power dissipated ($P_D/P_A$) is the same in both forward and reverse bias, then the minimum for this ratio is that shown in Table 2.

Generally, the choice of circuit that would provide the maximum power stresses to the diode is not the same choice that would produce equal power dissipation in its two states, but the two limits are very useful for estimating what performance limits a practical circuit might incur. Furthermore, since phase shifter bits are usually designed for low loss, the average of the losses in the two bias states is about equal to the minimum value specified in Table 2. The loss so calculated is for *pin* dissipation only. Circuit losses add to this value; but, as will be shown, a practical 3 -bit, L band phase shifter can be made with less than 1 dB of total insertion loss.

If the series resistance of the *pin* is about the same in both bias states ($R_F = R_R$), an equal loss phase shifter can be made by installing the *pin* at the 3 dB outputs of the coupler with a series inductance whose reactance magnitude is half that of the *pin*'s capacitive reactance. By installing a quarterwave transformer between coupler and diode termination (Fig. 18), the phase shift can be adjusted to any desired value, allowing use of the same *pin* and series inductance for all bits (Fig. 19).

The method for constructing the backward wave coupler (2) reflection phase shifter is shown in Figs. 20 and 21. A three-layer dielectric stripline sandwich is employed, wherein the center dielectric is used for the coupled lines. Using this

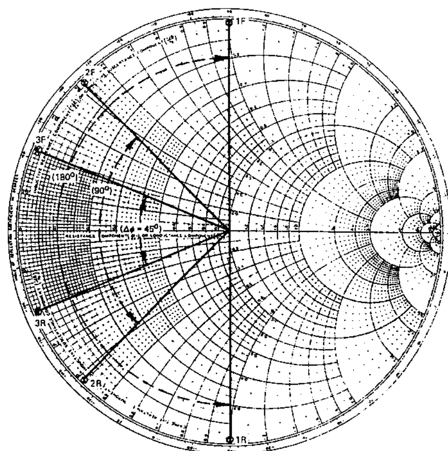

**Figure 19.** The reflection coefficients seen at the coupler for loss equalized 180°, 90°, and 45° phase shift bits.

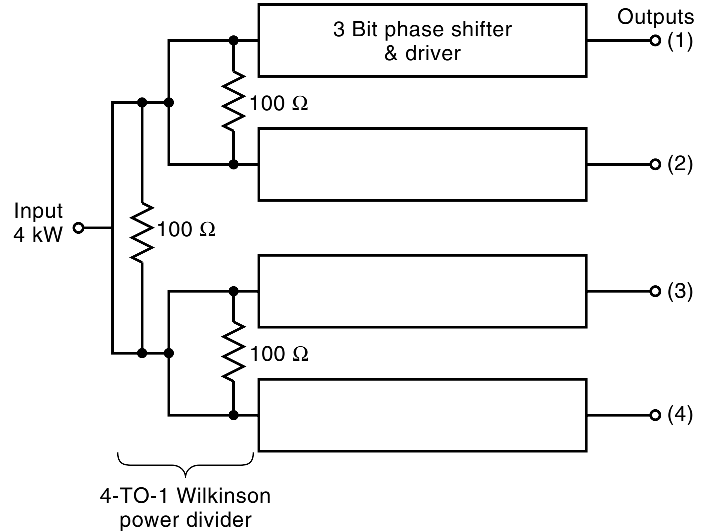


**Figure 20.** The 4-to-1 power divider and phaser assembly.

approach, a 3 bit phase shifter was designed for use in the Cobra Dane radar built for the US Air Force by the Raytheon Company on Shemya Island, near the western tip of the Aleutian Island chain. To minimize losses, the outer dielectrics were removed, resulting in air stripline in the transformer and diode regions. The operating bandwidth was approximately 1,200 MHz to 1,400 MHz and the required power handling capacity was to be 1 kW peak, with evenly spaced pulses of up to 2,000 $\mu$s and 0.05 duty cycle.

The schematic diagram for the unit is shown in Fig. 20. Four separate phase shifters and a Wilkinson equal-phase power divider were housed in a single assembly to reduce costs and interface connections. Figure 21 shows the diode mount detail, and measured performance is shown in Fig. 22. A photograph of the completed assembly is shown in Fig. 23.

The diode used for all bits was the 3 pF, 1,800 V bulk breakdown *pin* listed in the first column of Table 1. The individual phase shifter section, tested with −200 V bias on all diodes, sustained 4.1 kW to 4.8 kW peak power before burnout, and therefore could be rated for 1 kW operating level. The insertion loss of each phase shifter, including both *pin* diode and circuit losses, was 0.7 dB. About 16,000 phase shifters were installed in the Cobra Dane antenna array, which

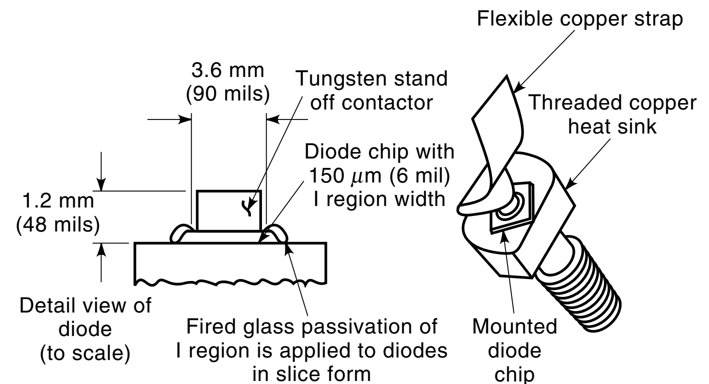


**Figure 21.** The high-voltage *pin* chip mounted on a copper heat sink.

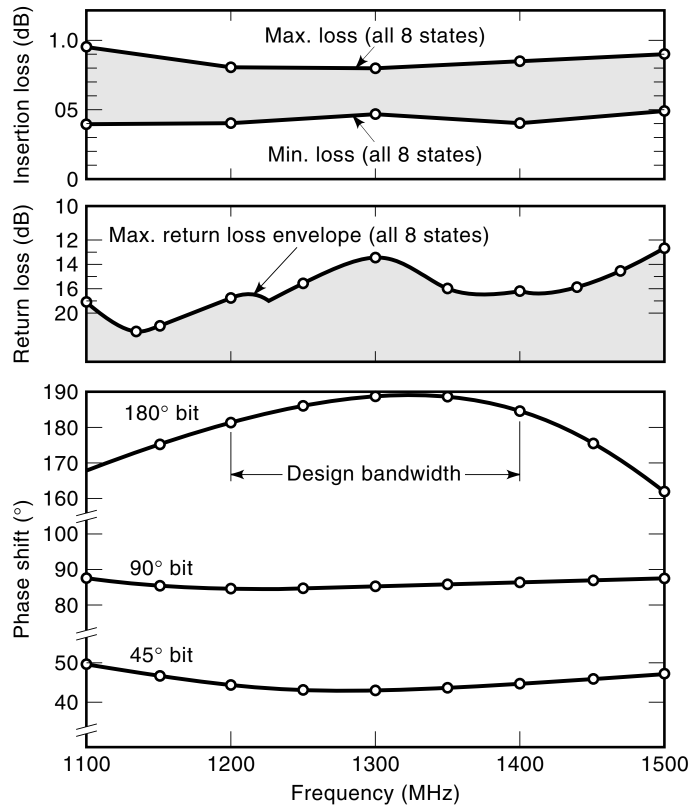


**Figure 22.** Measured performance for the L-band, 3-bit stripline phase shifter.

radiates approximately 16 MW peak and 1 MW of average power. At the time of installation the array was operated 20 h per day, resulting in nearly two million device hours daily.

In separate projects, *pin* phase shifters of 3- and 4-bit designs were implemented at S, C, and X bands [(2), Chap. 6]. C band phasers find use in the scanning beam Microwave Landing System (MLS), for which a worldwide standard exists. Generally, higher-frequency diode phasers have progressively higher insertion loss and lower peak power capacity. At X band, the 4-bit design had 2 dB of insertion loss and a burn-

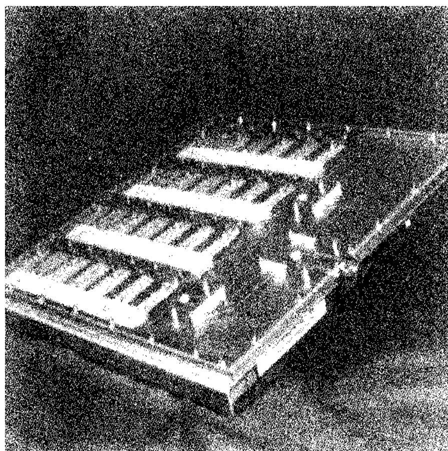

**Figure 23.** Photograph of the Cobra Dane 4-to-1 divider and high-power phase shifter assembly.

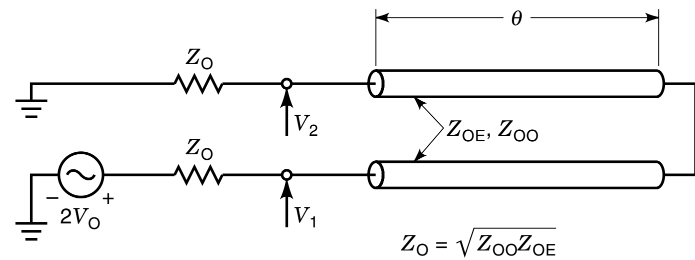


**Figure 24.** Schiffman phase shift section.

out power of about 1,000 W with 1 $\mu$s pulse lengths and 0.001 duty cycle.

## CONSTANT PHASE SHIFT WITH FREQUENCY

Frequently there is a need for a phaser whose phase shift is constant over a considerable bandwidth. Schiffman (2,4) observed that when the backward wave coupler has ports 2 and 4 connected to each other (Fig. 24), an all-pass network results, having a dispersion characteristic (an electrical length which does not increase linearly with frequency) that can be adjusted with the coupling coefficient (Fig. 25).

A switched path phase shifter (Fig. 26), which alternates between a Schiffman section and a uniform transmission line of appropriate length, can be made to have a nearly constant phase shift over an octave bandwidth (Fig. 27).

## VARACTOR DIODE, CONTINUOUS PHASE SHIFTER

The varactor diode, lacking a wide I region, consists only of a *pn* junction, whose capacitance at RF frequencies is variable over a 5 to 1 or wider range with the application of a reverse bias. Such a variable reactance can be used in place of the *pin* in the reflection phase shifter circuit, to provide phase control which varies continuously with applied bias voltage. Of necessity, the continuous phase shifter is limited to low power, below 1 W, since the varactor capacitance can change at the RF rate. In fact, varactors are used as the nonlinear element in frequency multipliers.

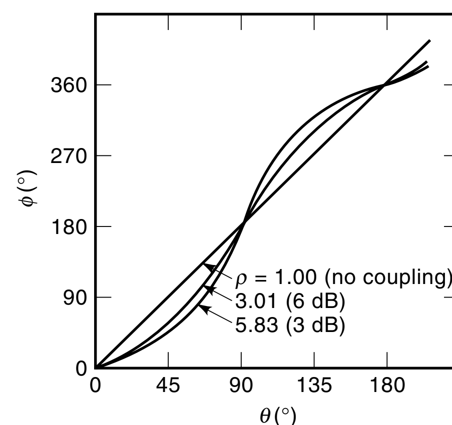


**Figure 25.** Dispersion characteristic of the Schiffman section.

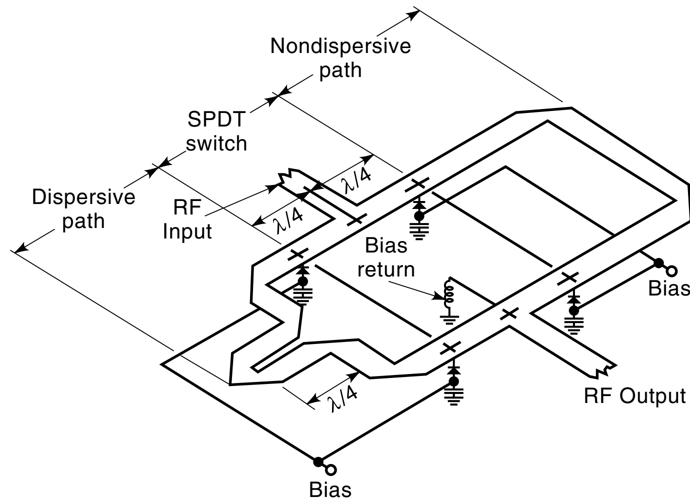


Figure 26. A stripline Schiffman phase shifter using diode path switching [after Grauling and Geller (5)].

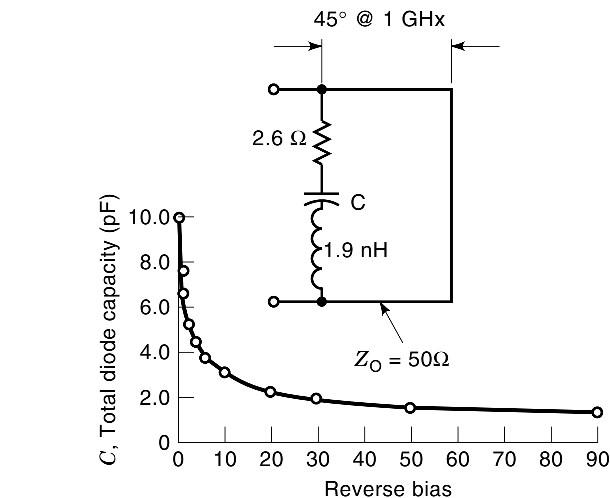


Figure 28. Representative varactor diode capacitance and circuit termination for a varactor continuous-phase shifter.

For varactor phase shifters, a figure of merit, $F$, applies [(2), p. 486], relating the number of degrees of phase shift per decibel of loss to the cutoff frequency of the varactor, $f_C = 1/2\pi RC_{MIN}$, where $C_{MIN}$ is the minimum capacitance obtained at a reverse bias just before the breakdown voltage, $V_B$; $M$ is the ratio of the capacitance at zero volts to that at $V_B$; and $f$ is the frequency of operation.

$$F = (f_C/f)(1 - 1/M)(6.6^\circ/\text{dB}) \tag{10}$$

This equation applies when the loss is small, below 1 dB. Thus a varactor having a junction capacitance which varies from 10 pF to 2 pF in series with a 2.6 Ω resistance (Fig. 28) has a cutoff frequency of 159 GHz and could yield 323°/dB at 1 GHz. Circuit losses must be added to this value.

Generally, higher loss is obtained due to the tuning effect of the varactor's series inductance and the circuit reactance employed to transform the reflection coefficient into a range which covers both the upper (inductive) and lower (capacitive) halves of the Smith Chart (Figs. 29 and 30).

The varactor phase shifter experiences little variation with temperature, typically only a one-percent change in total

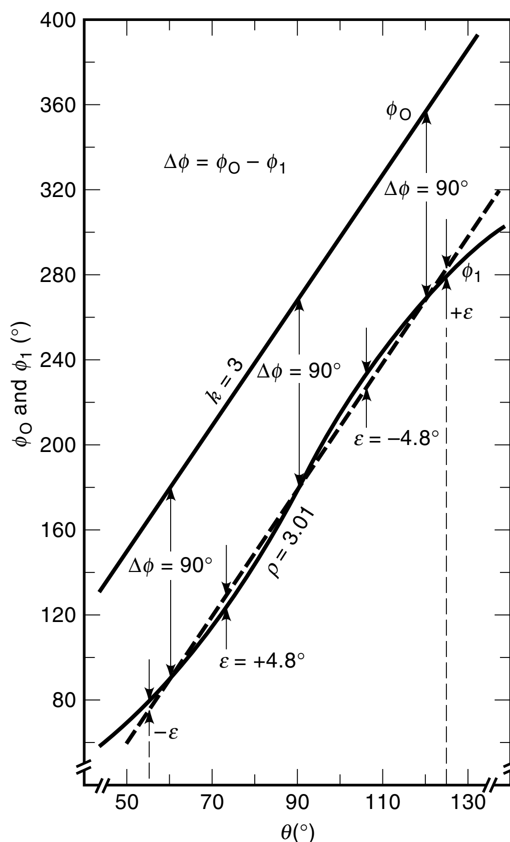


Figure 27. The octave bandwidth Schiffman phase shifter formed by a $\rho = 3.01$ (2) coupled line pair $\theta$ long and a uniform line path 3 $\theta$ long. Phase shift is 90° ± 4.8° for 55° ≤ $\theta$ ≤ 125°, a 2.24 : 1 frequency ratio.

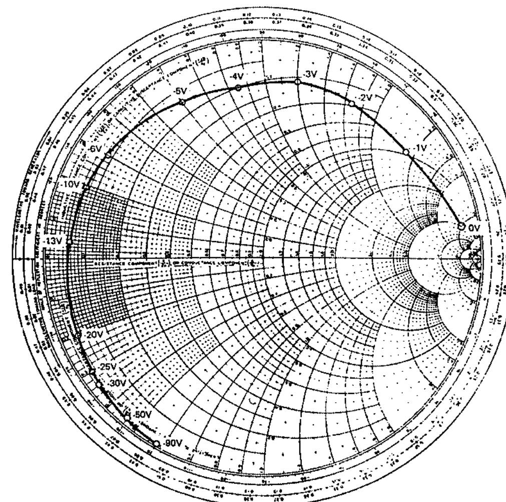

Figure 29. Phase shift (change in reflection coefficient angle) and loss (departure from unity reflection coefficient magnitude) of varactor circuit in Fig. 28.

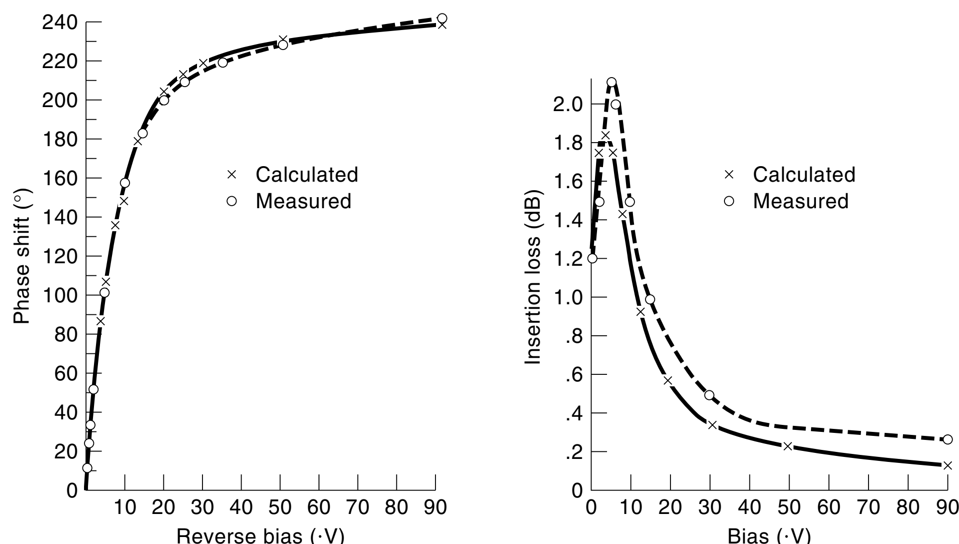


**Figure 30.** Calculated and measured phase shift and insertion loss at 1 GHz for the varactor termination of Fig. 27.

phase shift over a 50°C temperature change. Even this small change may be attributable to circuit changes and possibly could be reduced further. However, variations in RF power beyond one watt produce significant changes, particularly near zero bias, at which the applied RF voltage swings into the forward conducting region (Fig. 31).

## THE FET AS A SWITCHING DEVICE

Actually, any electronically switched device can be used as the control element in a phase shifter so long as it has sufficient $Q$ to provide acceptably low insertion loss. The considerable strides made in the development of field effect transistors (FETs) both for microwave power generation and switching [12–18] have two important implications for semiconductor phase shifting.

First, phase shifting for array antennas can be performed at low power levels with subsequent amplification by FETs and other solid state devices to the required output level at the array antenna radiating element. With this approach the achievement of lowest insertion loss is less critical. Of course, the amplification generally will be nonreciprocal, requiring that switching be performed between transmission and reception modes.

Second, the phase shifter can be realized using FET elements for switching instead of *pin* diodes. FET switches have an inherent advantage when compared to *pin* diodes in that the FET has a third (gate) terminal to which bias is applied, simplifying the design of the microwave circuitry in which bias blocking otherwise is needed for two terminal control elements.

FETs can be modeled as a lossy capacitor in the nonconducting state and a resistor in the conducting state, essentially the same equivalent circuit format used for the PIN diode. As a result, most of the formation developed for the *pin* can be used directly with FETs. The FET switched phase shifter can be reciprocal, as is the pin phase shifter.

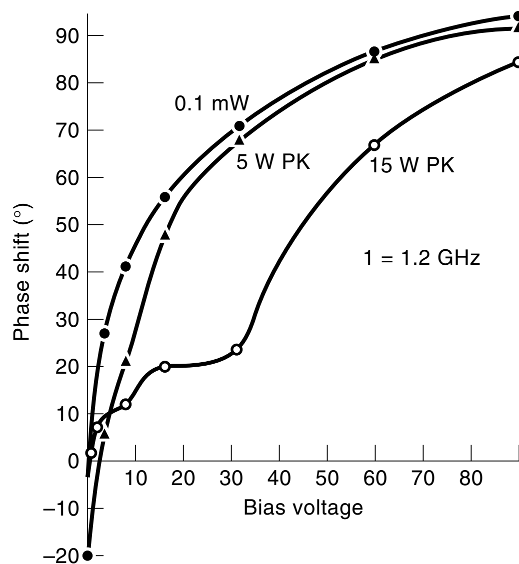


**Figure 31.** Typical variation of phase shift with RF input power.

## ACKNOWLEDGMENT

The contents of this article have been excerpted, with permission, from the author's text, *Microwave Semiconductor Engineering* (2). The author thanks Randy Rhea and Gary Breed for this opportunity. The phase shifter development described took place at M/A-COM, formerly Microwave Associates,and now a division of AMP, Inc., located in Burlington, Massachusetts. Much of the development of both the *pin* and varactor diodes, as well as the circuits to exploit them, was sponsored by the US Government through its Air Force, Navy, and Army research agencies.

## BIBLIOGRAPHY

1. R. Ryder, Bell Telephone Labs, Murray Hill, NJ, in a talk given at the NEREM Conference in Boston, MA, circa 1970.
2. J. F. White, *Microwave Semiconductor Engineering,* Tucker, GA: Noble Publishing, (Originally published under the title *Semiconductor Control,* Norwood, MA: Artech House, 1977. Later repub-

lished under the current title by Van Nostrand Reinhold Co., New York, 1982, and translated with permission into Japanese.)

3. M. E. Hines, Fundamental limitations in RF switching and phase shifting using semiconductor diodes, *Proc. IEEE,* **52**: 697–708, 1964.
4. B. M. Schiffman, A new class of broadband microwave 90° phase shifters, *IEEE Trans. Microw. Theory Tech.,* **MTT-6**: 232–237, 1958.
5. C. H. Grauling and B. D. Geller, A broadband frequency translator with 30 dB suppression of spurious sidebands, *IEEE Trans. Microw. Theory Tech.,* **MTT-18**: 651–652, 1970.
6. W. J. Ince and D. H. Temme, Phasers and Time Delay Elements, in L. Young (ed.), *Advances in Microwaves,* **4**, Academic Press, 1969, pp. 1–189.
7. I. Bahl and P. Bhartia, Microwave Solid State Circuit Design, New York: Wiley, 1988, chaps. 8, 13.
8. J. F. White, Semiconductor Control Devices: PIN Diodes, in K. Chang (ed.), *Handbook of Microwave and Optical Components,* vol. 2, New York: Wiley, 1990, chap. 4.
9. A. I. Sreenivas and R. Stockton, Semiconductor Control Devices: Phase Shifters and Switches, in K. Chang (ed.), *Handbook of Microwave and Optical Components,* vol. 2, New York: Wiley, 1990, chap. 5.
10. S. Yngvensson, *Microwave Semiconductor Devices,* Norwell, MA: Kluwer, 1991, chap. 9.
11. K. Chang, *Microwave Solid State Circuits and Applications,* New York: Wiley, 1994, chap. 8.
12. A. Mallet-Guy et al., Modeling and performance of a sub-nanosecond high isolation DC-18 GHz monolithic SPST with driver, *IEEE MTT-S Int. Microw. Symp. Dig.,* **1**: 193–196, 1991.
13. H. Takasu et al., GaAs FET switch model for X-band MMIC phase shifter design, *1994 IEEE MTT-S Int. Microw. Symp. Dig.,* **3**: 1413–1416, 1994.
14. M. J. Schindler and T. E. Kazior, High power 2-18 GHz MMIC TR switch, *Appl. Microw. Mag.,* Summer: 90–94, 1991.
15. F. McGrath et al., Multi gate FET power switches, *Appl. Microw. Mag.,* Summer: 77–86, 1991.
16. T. Tokumitsu, I. Toyoda, and M. Aikawa, Low voltage, high power T/R switch MMIC using LC resonators, *IEEE Microw. Millimeter-Wave Monolithic Circuits Symp. Dig.,* June: 27–30, 1993.
17. A. Ehoud et al., Extraction techniques for FET switch modeling, *IEEE MTT-S Trans.,* August: 1863–1867, 1995.
18. K. Purnell et al., GaAs MESFET, passive element, MMIC phase shifter, *IEEE Int. Microw. Symp. Dig.,* **2**: 1197–1200, 1996.

JOSEPH F. WHITE
JFW Technology, Inc.

**MICROWAVE PHASE SHIFTERS.** See FERRITE PHASE SHIFTERS.

**MICROWAVE POWER APPLICATIONS.** See MICROWAVE HEATING.